Diffusion-Controlled Elementary Reactions in Tubular Confinement: Extreme Nonclassicality, Segregation, and Anomalous Scaling Laws for Dimensional Crossovers

Anna L. Lin[†] **and Raoul Kopelman***[,‡]

Department of Chemistry, University of Michigan, Ann Arbor, Michigan 48109-1055

Panos Argyrakis[§]

Department of Physics, University of Thessaloniki, 54006 Thessaloniki, Greece

Received: September 19, 1996[⊗]

To understand reaction kinetics in capillaries, pores, and tubules, we performed Monte Carlo simulations of random walk based exploration volumes and bimolecular A + A and A + B reactions on baguette-like lattices. The emphasis is on the scaling of the dimensional crossover times with tube width. We find that the exponents range between 1 and 4, i.e., that the global information propagates either slower or faster than single-particle diffusion, depending on the reaction type (e.g. A + A or A + B) and on the dimensionality (2 or 3). The time evolutions of the A + A reactions approximately mimic those of the average exploration volumes, within the simulation uncertainties. All asymptotic time behaviors exhibit truely one-dimensional character, i.e., extremely nonclassical kinetics. Rapid and complete A, B reactant segregation is illustrated. The nonuniversal scaling powers present a new theoretical and experimental challenge.

1. Introduction

Due to the general absence of convection inside tubules, pores, and capillaries, the observable rate laws for elementary chemical reactions that may occur within such quasi-one-dimensional structures are expected to exhibit nonclassical diffusion-controlled reaction kinetics. Nonclassical reaction kinetics with one-dimensional rate-law characteristics have been clearly demonstrated experimentally for several systems,[1−3] including bimolecular reactions in solution-filled pores[4,5] and binary exciton annihilation in crystalline media embedded inside pores,[6−8] as well as for exciton annihilation on isolated guest chains[9] in polymer blends. While the dynamics of diffusion-controlled photochemical and photophysical processes indicated a fractal-like network structure in some of these systems, most of the systems studied, including the well-characterized nuclepore membranes,[2] revealed cylindrical pore structures. These cylindrical systems exhibited crossover times dependent on width or, alternatively, crossover widths for given experimental time scales.

The nonclassical, anomalous behavior of the A + *A* elementary reaction[1−14] has been shown[3,8−12] to be caused by the anomalously large and continuously growing kinetic depletion zones, i.e., fluctuating mesoscopic domains, where the reactants have been depleted. Even more dramatic nonclassical effects have been demonstrated for elementary A + B reactions[3,15−18] where kinetic self-segregation between A and B, the Ovchinnikov−Zeldovich effect,[15] has been demonstrated for an initially random system, as well as for steady state conditions.[19,20] This purely kinetic self-segregation of reactants in an elementary reaction has not yet been observed experimentally. Only the related Racz[21] effect—the preservation of the segregation front for A + B reactions with initially separated reactants, has been observed in laboratory experiments on reactions in capillaries.[22,23] The Ovchinnikov−Zeldovich rate law deviates from classical kinetics only slightly in three dimensions, more in two, and most prominently in one dimension. In addition, the Ovchinnikov−Zeldovich effect is "wiped out" by convection or reversibility. Convection is difficult to avoid in three dimensions; the degree of convection sufficient to thwart the Ovchinnikov−Zeldovich effect is highest in three dimensions and lowest in one dimension; i.e., this effect is most "fragile" in three dimensions. Therefore, one-dimensional experimental realizations should yield the clearest results. While strictly one-dimensional reaction systems are hard to come by experimentally, it is much easier to find or to construct systems that are effectively one-dimensional—capillaries, pores, or tubules, for example. Such systems are, or can be made to be, immune to convection currents, and only a large degree of reaction reversibility can frustrate the Ovchinnikov−Zeldovich effect.[25] To encourage such experiments, we performed simulations of such tubular systems, using "baguette-like" lattices, with the aim of quantifying the conditions necessary for the observation of the Ovchinnikov−Zeldovich effect. Since in the short time regime (before the Ovchinnikov−Zeldovich effect is reached) the A + B reaction mimicks the behavior of the A + A reaction, we have also simulated the A + A case. Also, as the A + A reaction generally follows the scaling of the average exploration volume of a random walker,[18,24] we also simulated this case. For completeness, we have simulated two-dimensional "flat" tube reactions to compare with the three-dimensional tube results.

We note that classical reaction kinetics is dimension independent; therefore, its reaction orders and the time exponents describing the densities (survival probabilities) or reaction progress are dimension independent (see below). Thus, there are no time crossovers of the scaling laws. On the other hand, the dimensional sensitivity of nonclassical kinetics implies crossover times that depend on tube diameter. Previous work[16,25−27] has effectively used scaling arguments based on the mean square displacement law (Einstein diffusion) to describe the time dependence of diffusion-controlled reaction kinetics. The latter law has also been found[18,27] to describe correctly the crossover times for the onset of finite size effects in regular lattices (1, 2, and 3-D). Is this law also relevant to

[†] E-mail: alin@chem.lsa.umich.edu.
[‡] E-mail: kopelman@umich.edu.
[§] E-mail: argyrakis@physics.auth.gr.
[⊗] Abstract published in *Advance ACS Abstracts,* January 1, 1997.

S1089-5639(96)02890-3 CCC: $14.00

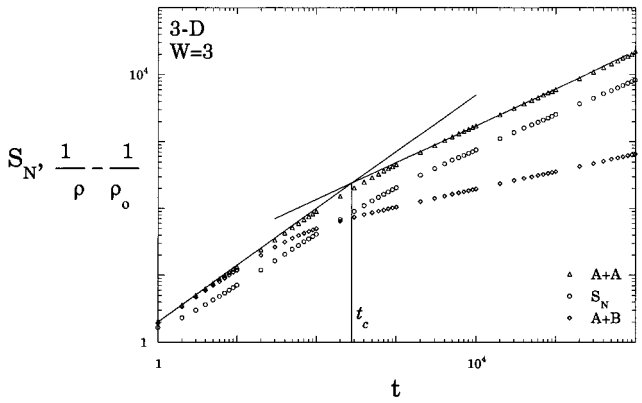

Figure 1. Representative data plots for three processes: S_N, the average number of distinct sites visited (200 runs averaged), and the reaction progress of both A + A → 0 (25 runs averaged) and A + B → 0 (7 runs averaged), as measured by $\langle\rho(t)\rangle^{-1} - \rho_0^{-1}$, vs time, all occurring on a spatially anisotropic, "baguette-like" lattice of size $3 \times 3 \times 10^5$. The initial density, ρ_0, is 0.8 particle/site for the A + A simulations and 0.4 in each species for the A + B process. The crossover time, t_c, from 3-D behavior at early times to 1-D behavior at asymptotic times is found from the intersection of the two solid lines, which are drawn as best straight line fits to the data at early and asymptotic times.

the crossover times due to the finite width of the tube? To answer this question and to help interpret existing experiments and to guide new ones, Monte Carlo simulations were performed for elementary A + A and A + B irreversible reactions and for the average exploration volume, in two- and three-dimensional baguette-like lattices. Seen in Figure 1 are data representing each of the three processes which we discuss in this paper: the number of distinct sites visited, S_N, the elementary reaction process A + A → 0, and the elementary reaction process A + B → 0. The latter two are both measured in terms of the reaction progress, $\langle\rho(t)\rangle^{-1} - \rho_0^{-1}$, where ρ_0 is the initial *A* particle density. In Figure 1 the solid line fits to the A + A data give an example of how we determined the crossover time, t_c, between the early time and asypmtotic time behavior.

We find that the crossover times, t_c, do scale with lattice width, but with unexpected powers. The exponents range between 1 and 4; i.e., the global information propagates either slower or faster than single-particle diffusion, depending on the reaction type (e.g., A + A or A + B) and on the dimensionality (2 or 3). At times well beyond the crossover time, the number of distinct sites visited, S_N, and both the A + A and the A + B reactions display the characteristic, asymptotic, nonclassical behavior of a one-dimensional system. Kinetic depletion zones develop for both reactions and spatial segregation of reactants occurs for the A + B reaction. Well before the crossover time some nonclassical behavior is observed as well, even for the effectively three-dimensional systems. No truely classical kinetic time regime is found for narrow tubes, irrespective of their length.

2. Method of Simulation

Monte Carlo computer simulations are often used to model random processes such as diffusion,[27−32] using a random number generator to simulate the random walk of a particle(s) on a lattice structure. The lattices on which we investigate the behavior of the number of distinct sites visited in time, S_N, the A + A → 0 reaction process and the A + B → 0 reaction process, are highly anisotropic—they have different linear sizes in the *x* and *y*, compared to the *z*, dimensions. Typically, for the 2-D case *x* is small, varying from $x = 3$ to 50, while *y* is long, typically 10^5-10^6 sites. For particle diffusion in the *x* dimension, we used reflective boundary conditions, which means that the particles are reflected if they reach the ends of the lattice in the *x* dimension. In the *y* (long) dimension we use cyclic boundary conditions, which means that if the particles reach the ends of the lattice in the *y* dimension, they continue their motion at the other end of the lattice. For the 3-dimensional, baguette-like lattices, usually *x* and *y* are small (and $x = y$), with reflective boundary conditions, while *z* is the long dimension, with cyclic boundary conditions. The actual sizes used for the long dimension are such that, in the calculation of S_N, a particle starts in the middle of the lattice and the boundaries in the long dimension are never reached. The different boundary conditions used in the various dimensions add to the anisotropic character of the particle motion.

In the course of reflection at the walls along the short dimension(s), one can choose from two different approaches for the calculation of time, a situation that frequently appears in similar problems. A reflection at the boundary may or may not consume one time unit (one Monte Carlo step), leading to the so-called blind and myopic ant models, respectively. From past experience,[30,31] these models usually give similar answers for the exponents of the scaling laws, even though the absolute values of the monitored parametrs are different. We used both models in the present study. Most calculations were performed with the blind ant model, but several cases were checked with the myopic ant model as well. The scaling results are the same.

Our computer simulations for diffusion-limited chemical reactions are performed according to the following algorithm. A population of reacting particles is initially placed on a lattice by randomly choosing the coordinates for each particle. Particles move by diffusion on the lattice, which is modeled by independent random walks of the individual particles, one at a time. The coordinates of all particles are monitored as a function of time. Steps are allowed to nearest-neighbor sites only. There is no interparticle interaction. Reaction occurs, for the A + A type reaction, if two A particles "collide", i.e., two A's attempt to occupy the same lattice site. Every collision leads to a reaction with a probability of one, and excluded volume conditions are maintained. When two particles react in this fashion, they are removed from the system (they are annihilated). Time is advanced one unit after all particles still present on the lattice have attempted to move once.

For the A + B type reaction, reaction occus when an A and a B particle collide. No reaction occurs if two *A* particles (or two *B* particles) collide. If an A(B) particle attempts to land on a site already occupied by another A(B) particle, the particle does not move in that time step (excluded volume condition). Every collision of an *A* particle with a *B* particle leads to a reaction with a probability of one, and both particles are removed from the system (annihilated).

In this study we only treat "batch reactions", i.e., the case where all reactants are generated at time zero, before any reaction has occurred, and thus the particle density decreases as a function of time. The width and height of the three-dimensional lattices are chosen to be equal so that the two- and three-dimensional cases can be more easily compared.

3. Results and Discussion

It has been shown[3,10,32,33] that diffusion-limited reaction processes are intimately related to the behavior of the average number of distinct sites visited by a single random walker, S_N, as a function of time (N = time). Thus, to better understand the behavior of diffusion-limited elementary reaction processes on spatially anisotropic lattices, we first studied the behavior of S_N on such lattices, using Monte Carlo simulation techniques to model a single random walk on spatially anisotropic (baguette-like) lattice structures.

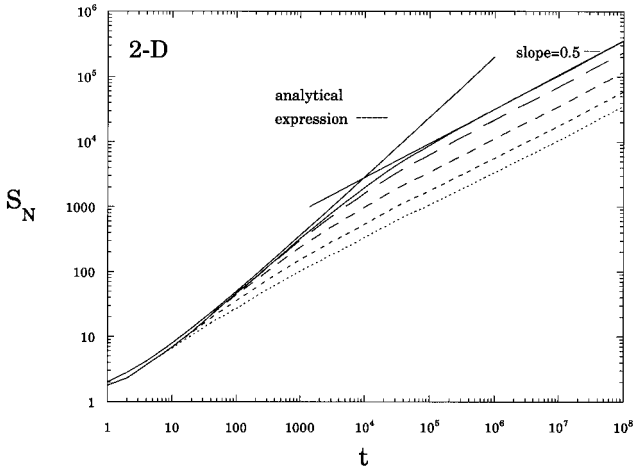

Figure 2. Number of distinct sites visited, S_N, on spatially anisotropic 2-D lattices, plotted as a function of time. Simulations were done on 3 $\times$ 10^6, 5 $\times$ 10^6, 10 $\times$ 10^6, 20 $\times$ 10^6, and 30 $\times$ 10^6 site lattices (bottom to top lines, respectively). The analytical formula of Henyey and Seshadri (eq 5) for S_N in 2-D and a line with slope 0.5 are plotted, as solid lines, to illustrate how the crossover time, t_c, was measured.

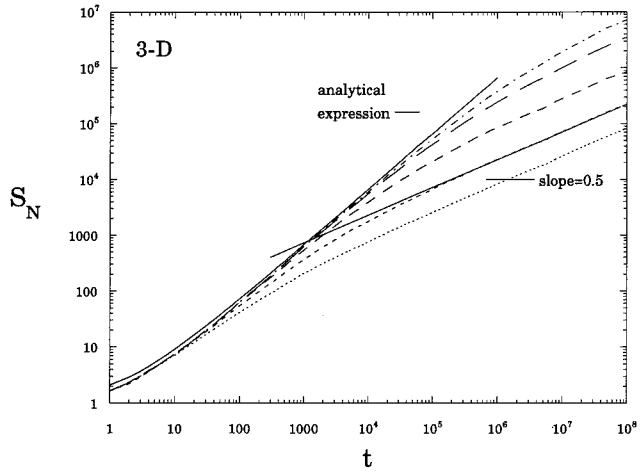

Figure 3. Number of distinct sites visited, S_N, on spatially anisotropic 3-D lattices, plotted as a function of time, for 3 $\times$ 3 $\times$ 10^5, 5 $\times$ 5 $\times$ 10^5, 10 $\times$ 10 $\times$ 10^5, 20 $\times$ 20 $\times$ 7500, and 30 $\times$ 30 $\times$ 5000 site lattices, shown by dotted and/or dashed lines (bottom to top, respectively). The analytical formula of Montroll and Weiss (eq 6) for S_N in 3-D and a line with a slope of 0.5 are plotted, as solid lines, to illustrate how the crossover time, t_c, was measured.

The analytical expression for S_N in the asymptotic limit of $N \rightarrow \infty$, where N is the number of steps, has been given by Montroll and Weiss[34] for all three dimensionalities. In 1-D, S_N follows a $t^{1/2}$ power law, in 3-D it is linear with t, and in 2-D it is "almost" linear, with an additional logarithmic term:

$$S_N \sim \left(\frac{8N}{\pi}\right)^{1/2} \qquad N \rightarrow \infty \qquad \text{1-D} \qquad (1)$$

$$S_N \sim \frac{\pi N}{\log(N)} \qquad \text{N} \rightarrow \infty \qquad \text{2-D} \qquad (2)$$

$$S_N \sim N \qquad \text{N} \rightarrow \infty \qquad \text{3-D} \qquad (3)$$

These are the asymptotic equations. Correction terms, which add accuracy to the early time behavior, have also been derived. We use the analytical expressions 2 and 3, with their associated correction terms[34,35]

1-D:

$$S_N = \left(\frac{8N}{\pi}\right)^{1/2}\left\{1 + \frac{1}{4N} - \frac{3}{64N^2} + ...\right\} \qquad (4)$$

2-D:

$$S_N = \frac{AN}{\ln(BN)}\sum_{j=0}^{\infty}\frac{-\delta_\beta^{\,j}}{\ln BN}|_{\beta=2}\left[1 + \text{O}\left(\frac{1}{N}\right)\right] \qquad (5)$$

3-D:

$$S_N = 0.65946267N + 0.573921N^{1/2} + 0.449530 + 0.40732N^{-1/2} + ... \qquad (6)$$

where A and B in eq 5 are constants. We implement eqs 5 and 6 to compare the behavior of S_N on isotropic lattices to that observed on our anisotropic, baguette-like lattices at early times. We also use eqs 1, 5, and 6 to determine the crossover time, t_c, of S_N from 3-D or 2-D behavior, into 1-D behavior, as discussed below.

The number of distinct sites visited, S_N, as a function of time, for a single random walker on baguette-like lattices with $W \times L$ or $W \times W \times L$ sites, where $W \ll L$, is plotted in Figures 2 and 3, respectively, for 2- and 3-D. We do observe a crossover in S_N from 2- or 3-D behavior (depending on the embedding space), at early times, to a 1-D behavior asymptotically. The early time behavior of S_N on these baguette-like lattices indeed follows that found in 2(or 3)-D, as can be seen by its adherence at early times to the respective analytical formulae, eqs 5 and 6, while its long time behavior shows the characteristic 1-D slope of 0.5 on a log$-$log plot, as expected from eq 1.

The single random walker simulations were done on baguette-like lattices with ample lengths, such that site revisitations, due to finite size effects, did not occur in the length direction. The single random walker might be expected to experience the short boundaries (i.e., the width), and thus the 1-D character of the lattice, in a time that scales as $t_c \sim W^2$, following the mean square displacement law. To test this hypothesis, or any other scaling law, we derived the crossover times from high (2-, 3-) to low (1-) dimensional behavior as a function of lattice width.

In the method which we employ to find t_c for the S_N curves, we use the analytical expression of eq 5 or 6, respectively, as the early time fit to the 2- or 3-D data and a line with a slope = 0.5 to fit the asymptotic data. The time axis value corresponding to the intersection of these two fits to the data is defined as t_c (see Figures 2 and 3). The other method, which we employ to determine the crossover time, t_c, for the A + A $\rightarrow$ 0 and A + B $\rightarrow$ 0 processes, involves drawing "best" linear fits to both the early time and the asymptotic time portions of the curve. Again, the corresponding time axis value where these two straight lines intersect is defined as t_c (see Figure 1). Both of these methods are used to determine crossover times for the A + A $\rightarrow$ 0 process (since the behavior of the A + A process maps that of S_N, one can utilize the analytical expressions for the behavior of S_N in 2- or 3-D to fit the early time A + A behavior as well). While the absolute values for t_c obtained from these two methods are different, the resulting scaling relation between t_c and W is the same for a given process, within the associated error.

Figures 4 and 5 show the time evolution of the reaction progress, $\langle\rho(t)\rangle^{-1} - \rho_0^{-1}$, for the A + A $\rightarrow$ 0 process on 2-D and 3-D baguette-like lattices, respectively. The A + A $\rightarrow$ 0 reaction progress, measured by $\langle\rho(t)\rangle^{-1} - \rho_0^{-1}$, has been found before[3,14,18] to map, in time, the number of distinct sites

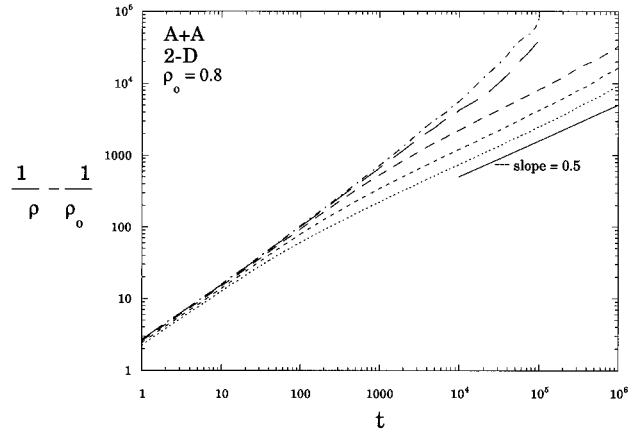

Figure 4. Reaction progress, $\langle\rho(t)\rangle^{-1} - \rho_0^{-1}$, vs time, plotted for the A + A → 0 reaction occuring on spatially anisotropic 2-D lattices of the same sizes as those decribed in the caption of Figure 2. The initial A particle density was 0.8 particle/site in all cases. Note the slope = 0.5 line and that the long time data show some finite length effects.

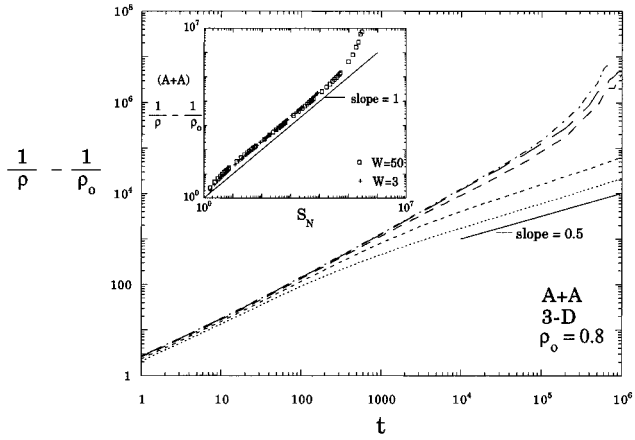

Figure 5. Reaction progress, $\langle\rho(t)\rangle^{-1} - \rho_0^{-1}$, vs time, plotted for the A + A → 0 reaction occuring on spatially anisotropic 3-D lattices of the same sizes as those decribed in the caption of Figure 3. The initial A particle density was 0.8 particle/site in all cases. Note the slope = 0.5 line and that the long time data exhibit some finite length effects. The inset figure shows the linear correspondence between the behavior of S_N and the A + A → 0 reaction on spatially anisotropic lattices of size $3 \times 3 \times 10^5$ and $50 \times 50 \times 10^3$ over almost all (except very early and very late) times.

visited on spatially isotropic lattices, in both Euclidean and fractal dimensions. Comparing Figures 4 and 5 with Figures 2 and 3, we find that this mapping persists on spatially anisotropic lattices. The inset in Figure 5 shows this correspondence of the progress of the A + A → 0 reaction with S_N, since the plots of $\langle\rho(t)\rangle^{-1} - \rho_0^{-1}$ for the A + A → 0 reaction vs S_N, on $3 \times 3 \times 10^5$ and $50 \times 50 \times 1000$ site baguette-like lattices, do result in lines with slopes of approximately 1. (While, for low initial densities, the very early time behavior of the A + A → 0 reaction is classical and then crosses over to the anomalous A + A behavior (resulting from the buildup of depletion zones around A particles[8]), we do not really see this in our high initial density simulations.) For $\rho_0 = 0.8$ particle/site, the initial density used in all of the A + A simulations, the crossover to the so-called A + A regime[27] certainly occurs within the first few time steps, as has been found before for isotropic lattices with high initial densities. For all lattice sizes examined, the density plots of the behavior in both the 2-D and 3-D systems show an asymptotic slope of 0.5, i.e., a crossover to the 1-D behavior.

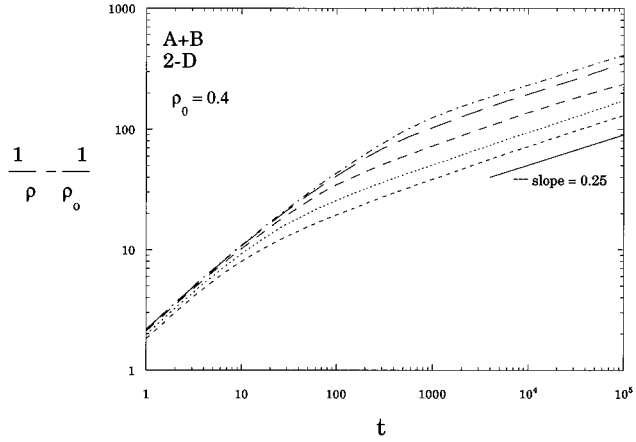

Figure 6. Reaction progress, $\langle\rho(t)\rangle^{-1} - \rho_0^{-1}$, vs time, plotted for the A + B → 0 reaction occuring on spatially anisotropic 2-D lattices of the same sizes as those decribed in the caption of Figure 2. In all cases, the initial A and B particle densities were 0.4 particle/site for each species. Note the slope = 0.25 line.

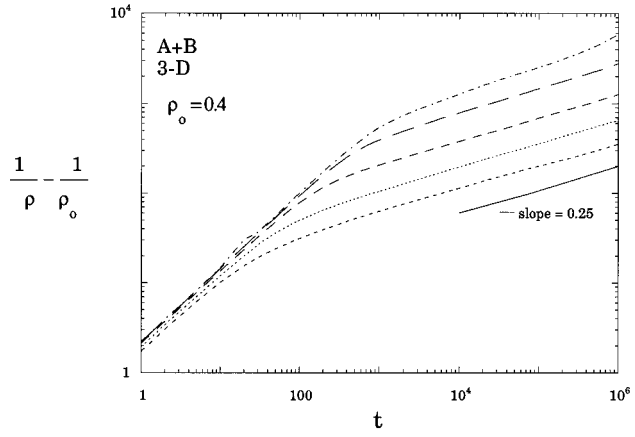

Figure 7. Reaction progress, $\langle\rho(t)\rangle^{-1} - \rho_0^{-1}$, vs time, plotted for the A + B → 0 reaction occuring on spatially anisotropic 3-D lattices of the same sizes as those decribed in the caption of Figure 3. In all cases, the initial A and B particle densities were 0.4 particle/site for each species. Note the slope = 0.25 line.

The reaction rate of the A + B → 0 process occuring on baguette-like 2- and 3-D lattices was followed by measuring $\langle\rho(t)\rangle^{-1} - \rho_0^{-1}$ vs time, and the results are plotted in Figures 6 and 7. All simulations were run with the intial condition $\rho_0 = \rho_A = \rho_B$. From these plots we observe a crossover of the reaction process, from a behavior characteristic of 2- or 3-D, to the asymptotic behavior that is expected if the binary A + B → 0 reaction process occurs in a truely 1-D space. Specifically, we find the expected[15,16,26] asymptotic 1-D slope of 0.25 on a log−log plot. For the A + B → 0 reaction, the time dependent behavior of the reaction progress, $\langle\rho(t)\rangle^{-1} - \rho_0^{-1}$, does not map onto that of S_N, in contrast to the A + A → 0 reaction progress, except possibly at very early times.

In Figure 8, $\langle\rho(t)\rangle^{-1} - \rho_0^{-1}$ vs time is plotted for the A + B → 0 reaction occuring on baguette-like lattices of sizes $3 \times 3 \times 10^5$, $3 \times 3 \times 12\,000$, and $3 \times 3 \times 12\,000$ for three different initial densities: $\rho_0 = 0.1$, 0.2, and 0.4 particle/site, respectively. The inset in Figure 8 is a plot of the crossover time, t_c, vs W for the same three initial concentrations. The solid line in the inset plot has a slope of 1.4, the average of the three least-squares fits found for the scaling relation between t_c and W, for the three initial densities. It appears, from these results, that the scaling of the crossover time with the width of the lattice is independent of concentration (inset), while the actual crossover time is not, as can be seen in Figure 8, where higher initial

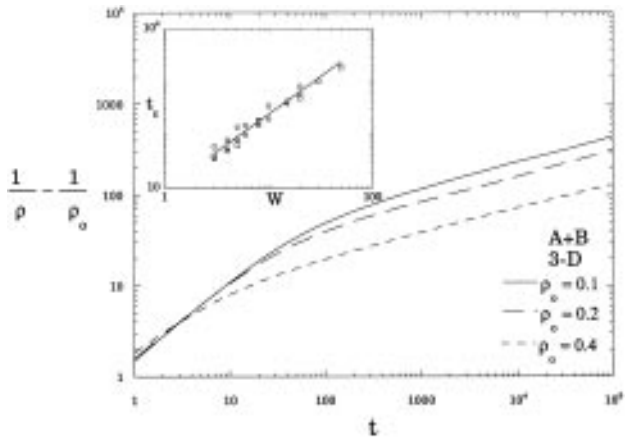

Figure 8. Reaction progress, $\langle\rho(t)\rangle^{-1} - \rho_0^{-1}$, vs time, plotted for three different initial densities of the A and B particles participating in the A + B → 0 reaction occuring on a $3 \times 3 \times 10^5$ site spatially anisotropic 3-D lattice. The inset figure shows the t_c dependence on width for the three densities: (○) $\rho_0 = 0.1$, (◇) $\rho_0 = 0.2$, and (□) $\rho_0 = 0.4$ particle/site, plotted in the main figure. The line plotted is an average of the least-squares fits to the three scaling curves and has a slope of 1.4.

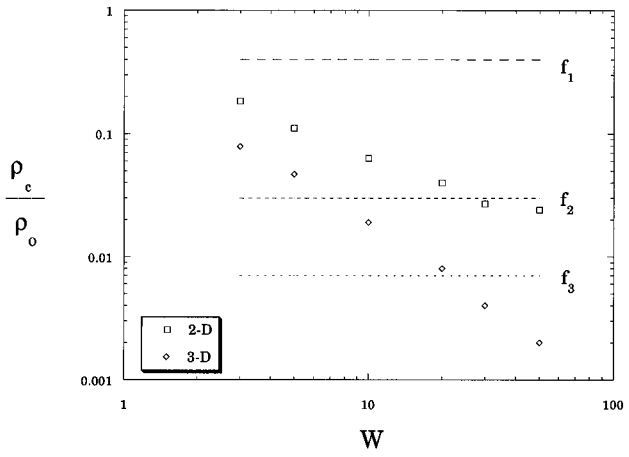

Figure 9. Density of particles remaining on the baguette-like lattice at the dimensional crossover time normalized by the initial particle density, ρ_c/ρ_0, as a function of lattice width, *W*. For comparison, the horizontal lines represent the normalized density of particles, f_d, remaining on a regular, isotropic lattice at the crossover to the Ovchinnikov−Zeldovich regime. The values of f_d, where *d* is the dimension 1, 2, or 3, are taken from refs 18 and 27.

densities exhibit a crossover to 1-D behavior more quickly than lower initial densities.

In Figure 9, we plot vs *W* the ratio ρ_c/ρ_0, which is the density of *A* particles remaining on the lattice at t_c, normalized by ρ_0, read from the data shown in Figures 6 and 7 for the A + B process occurring in 2- and 3-D, respectively. We note that, in general, $\rho(t)/\rho_0$ is the "survival probability", at time *t*, of the original particles. For comparison we plot another survival probability, ρ_c'/ρ_0, namely, the normalized densities at $t = t_c'$, where t_c' is the crossover time to the segregated (Ovchinnikov−Zeldovich) time regime in isotropic, linear, square, and cubic lattices found in earlier work,[18,27] where this ratio was called f_d ($d = 1, 2, 3$). These values are, of course, unrelated to the "baguette" width, *W*, in our baguette-like lattices and are represented in Figure 9 by horizontal, *W* independent lines, for $d = 1$, 2, and 3. From this plot one can observe that, for $W \leq 10$, the density ratios, ρ_c/ρ_0, at the times of the dimensional crossovers (t_c) in the 2- and 3-D baguette-like lattices, occur well above the density ratios needed for crossover into the Ovchinnikov−Zeldovich regime, given by $f_d = \rho_c'/\rho_0$, where *d* is the dimension of the isotropic lattice,[27] i.e., $t_c < t_c'$ for "thin baguettes". This implies that aggregates of like particles begin to form within the first few time steps on our narrow baguette-like lattices. This can be seen visually in our simulation movie snapshots of the A and B particles "diffusing" and "reacting" on 2-D "tube" lattices (see Figure 10). This aggregation seems to result in a slowing down of the reaction process and the deviation from the A + A type behavior (see Figure 1) in these baguettes, in contrast to the behavior observed for the A + B reaction, at early times, on isotropic lattices.[18,27]

In Figure 11, the crossover times, t_c, for S_N and for the reaction progress of the A + A → 0 and A + B → 0 reactions are plotted as a function of tube width, *W*, revealing the existence of scaling relations between these two parameters. The complex pattern of these scaling relations is possibly the most interesting behavior exhibited in these two- and three-dimensional tubelike lattices. We write this scaling relation in the form

$$t_c \sim W^x \tag{7}$$

where *x* is the crossover time scaling exponent. Table 1 lists these exponents. We see a dependence on both the dimensionality of the problem and the specific nature of the reaction. (Note that S_N represents directly some trapping reactions[32,33]). As mentioned previously, the absolute value of t_c for a given process on a certain lattice size can vary, depending on the method implemented for its determination. However, if each method is utilized in a self-consistent manner, the resulting scaling relations agree with each other, within the associated error (Table 1).

On the basis of an analogy to the finite size effect crossovers found for isotropic lattices,[18,27] one might have expected a universal crossover power of 2 in eq 7, i.e., $x = 2$ or $t_c \sim W^2$, in analogy to the Einstein mean square displacement diffusion law. Indeed, current arguments concerning both depletion zone growth in time (for trapping and A + A reactions) and aggregate size growth in time (for A + B reactions) are usually based on this mean square scaling law.[16,25−27,36] Furthermore, we note that in classical kinetics there is no dependence of any elementary reaction progress on dimensionality.[37] The reaction progress, measured by $\langle\rho(t)\rangle^{-1} - \rho_0^{-1}$, is simply linear in time at all times, and thus no crossover time can be defined (in a scaling sense).

In contrast to the above expectations, we see from Table 1 that even the simplest case, S_N, does not scale as the mean square displacement law ($x = 2$) but rather exhibits anomalous scalings on these 2- and 3-D spatially anisotropic lattices. Within the associated errors, the crossover times of the A + A → 0 reaction process follow (at least roughly) those of S_N. The A + A data are found only over a relatively narrow range of widths because the A + A reaction process occurs quickly in these baguette-like lattices and finite size effects set in (particle concentrations become too dilute) before the dimensional crossover can be reached for lattices with $W > 20$ in 2-D and for lattices with $W \geq 10$ in 3-D, approximately. We emphasize that the powers of S_N and of the 3-D A + A reaction are significantly larger than 2. This means that the information propagates slower than single-particle diffusion. Specifically, the start of the 1-D behavior requires the average particle to hit the tube wall repeatedly. On the other hand, the crossover powers for the A + B → 0 process are significantly smaller than two in both 2-D and 3-D baguette-like lattices. This result is surprising because it means that the information propagates faster than single-particle diffusion. Specifically, the start of the 1-D behavior does not require the average particle to hit the wall even once. The scaling of t_c with *W* appears to be universal on the length scales we studied—for both the small *W* lattices, where

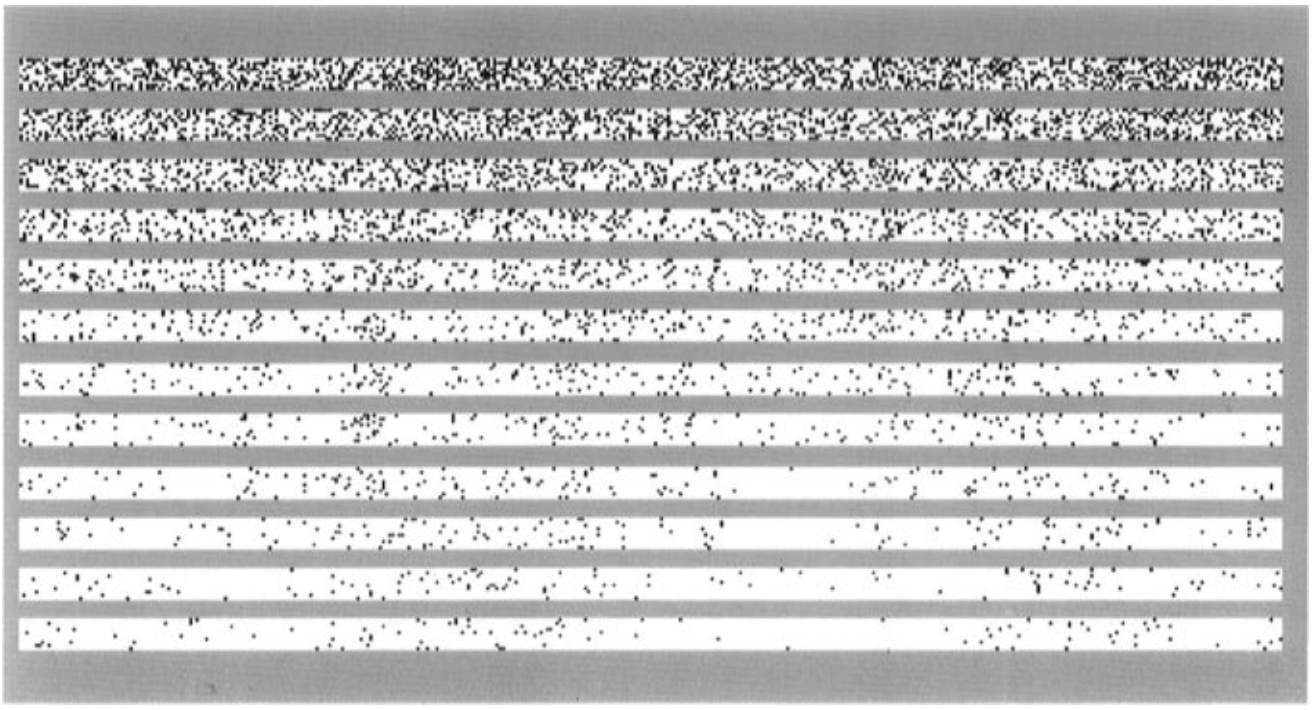

Figure 10. Time evolution of the A + B → 0 reaction on a 10 × 400 site lattice. The A and B particles are represented by blue and red pixels, and the underlying lattice space is represented with white pixels. One pixel equals one lattice site. The times corresponding to the snapshots of the reaction process shown here are (top to bottom) $t = 1$, 2, 4, 8, 16, 32, 64, 128, 256, 512, 1024, and 2048 steps. The initial particle density is 0.4 particle/site in each species. All particles remaining on the lattice move once within 1 time step.

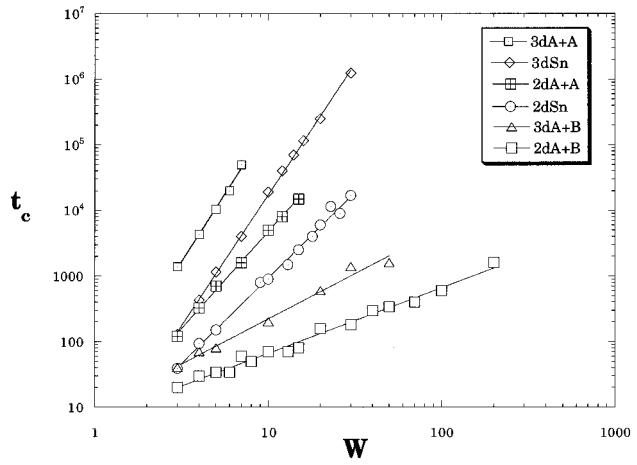

Figure 11. Plot of t_c vs W for S_N and for the progress of the two reactions, A + A → 0 and A + B → 0, on spatially anisotropic, "baguette-like" lattices, showing the scaling relation between the width, W, and the time, t_c, at which the process exhibits a crossover from its behavior in 2- or 3-D lattices to that in a 1-D lattice.

TABLE 1: Dimensional Scaling Exponents for the Relation between t_c and W (± Designates Estimated Accuracies)

	S_N	A + A	A + B
2-*D*	2.6 ± 0.4	2.8 ± 0.8	1.0 ± 0.2
3-*D*	4.0 ± 0.4	4.2 ± 1	1.4 ± 0.3

$\rho_c/\rho_0 > f_d$, and the large W lattices, where $\rho_c/\rho_0 < f_d$. We note that, while the precision of the scaling exponents is very high, the accuracy of these values (listed in Table 1) is less certain. Still, all but one of the values of these scaling exponents are well away from 2, presenting an unexpected result, with interesting theoretical and experimental implications.

4. Conclusions

Asymptotically, in the absence of finite size effects, all of the processes we have studied on the spatially anisotropic, tubular lattices do exhibit 1-D behavior. Had the diffusion process behaved classically in these baguette-like lattices, the power law relation between the reaction processes and time would have remained the same over all times, and there would have been no crossover between scaling laws. Instead, we observe a crossover in the temporal power law of these processes, and the time at which the crossover occurs does scale with lattice width. This scaling exhibits unusual exponents (different from 2), indicating that, depending on the process and the dimension of the embedding space, the information of the existence of a finite tube width propagates either faster or slower than expected for a purely diffusional mass transport process. The unexpected results discussed here present both a theoretical challenge and experimentally measurable phenomena.

Acknowledgment. This project was supported by NSF Grant No. DMR9410709 and by NATO Grant No. CRG920029 (to P.A.).

References and Notes

(1) *Molecular Dynamics in Restricted Geometries*; Klafter, J., Drake, J. M., Eds.; John Wiley and Sons: New York, 1989.
(2) *Nonequilibrium Statistical Mechanics in One Dimension*; Privman, V., Ed.; Cambridge University Press: Cambridge, U.K., 1996; Chapters 20 and 21.
(3) Kopelman, R. *Science* **1988**, *41*, 1620.
(4) Prasad, J.; Kopelman, R. *Chem. Phys. Lett.* **1989**, *157*, 535.
(5) Prasad, J.; Kopelman, R. *J. Phys. Chem.* **1987**, *91*, 265.
(6) Kopelman, R.; Parus, S. J.; Prasad, J. In *Excited State Relaxation and Transport Phenomena in Solids*; Skinner, J. L., Fayer, M. D., Eds.; *Chem. Phys.* **1988**, *128*, 209.
(7) Kopelman, R.; Parus, S.; Prasad, J. *Phys. Rev. Lett.* **1986**, *56*, 1742.
(8) Kopelman, R.; Parus, S. J.; Prasad, J. *Chem. Phys.* **1988**, *128*, 209.
(9) Kopelman, R.; Shi, Z.-Y.; Li, C. S. *J. Lumin.* **1991**, *48/49*, 143.
(10) Parus, S.; Kopelman, R. *Phys. Rev. B.* **1989**, *39*, 889.
(11) Doering, C. R.; Ben-Avraham, D. *Phys. Rev. A* **1988**, *38*, 3035.
(12) Doering, C. R.; Ben-Avraham, D. *Phys. Rev. Lett.* **1989**, *62*, 2563.
(13) Klymko, P. W.; Kopelman, R. *J. Lumin.* **1981**, *24/25*, 457.
(14) Klymko, P. W.; Kopelman, R. *J. Phys. Chem.* **1982**, *86*, 3686.
(15) Ovchinnikov, A. A.; Zeldovich, Y. G. *Chem. Phys. B* **1978**, *28*, 215.

(16) Toussaint, D.; Wilczek, F. *J. Chem. Phys*. **1983**, *78*, 2642.
(17) Lindenberg, K.; Romero, A. H.; Sancho, J. M.; Sagues, F.; Reigada, R.; Lacasta, A. M. *J. Phys. Chem*., in press.
(18) Lin, A.; Kopelman, R.; Argyrakis, P. *Phys. Rev. E*. **1996**, *53*, 1502.
(19) Anacker, L. W.; Kopelman, R. *Phys. Rev. Lett*. **1987**, *58*, 289.
(20) Lindenberg, K.; West, B. J.; Kopelman, R. *Phys. Rev. Lett*. **1988**, *60*, 1777.
(21) Galfi, L.; Racz, Z. *Phys. Rev. A* **1988**, *38*, 3151.
(22) Koo, Y. E.; Kopelman, R. *J. Stat. Phys*. **1991**, *65*, 893.
(23) Taitelbaum, H.; Koo, Y. E. L.; Havlin, S.; Kopelman, R.; Weiss, G. *Phys. Rev. A* **1992**, *46*, 2151.
(24) Lindenburg, K.; Seshadri, V.; Shuler, K.; Weiss, G. *J. Stat. Phys*. **1980**, *23* 11.
(25) Kang, K.; Redner, S. *Phys. Rev. A* **1985**, *32*, 435.
(26) Kang, K.; Redner, S. *Phys. Rev. Lett*. **1984**, *52*, 955.
(27) Argyrakis, P.; Kopelman, R.; Lindenberg, K. *Chem. Phys*. **1993**, *177*, 693.
(28) Ben-Avraham, D. *J. Chem. Phys*. **1988**, *88*, 941.
(29) Argyrakis, P. *Comput. Phys*. **1992**, *6*, 525.
(30) Havlin, S.; Ben-Avraham, D. *Adv. Phys*. **1987**, *36*, 695.
(31) Argyrakis, P.; Kopelman, R. *Phys. Rev. A* **1992**, *45*, 5814.
(32) Kopelman, R.; Argyrakis, P. *J. Chem. Phys*. **1980**, *72*, 3053.
(33) de Gennes, P. G. *C. R. Seances Acad. Sci., Ser. 2* **1983**, *296*, 881.
(34) Montroll, E. W.; Weiss, G. H. *J. Math. Phys*. **1965**, *6*, 167.
(35) Henyey, F. S.; Seshadri, V. *J. Chem. Phys*. **1982**, *76*, 5530.
(36) Leyvraz, F.; Redner, S. *Phys. Rev. A* **1992**, *46*, 3132.
(37) Levine, I. *Physical Chemistry*; McGraw-Hill Inc.: New York, 1982.